



# **$H \rightarrow Z\gamma$ Search and Photon Identification Efficiency Measurement in ATLAS Run-II**

Shuo Han, Institute of High Energy Physics, Chinese Academy of Science, China

September 8, 2015

## **Abstract**

The first part of this report presents some work about the search for a Higgs boson in the decay channel  $H \rightarrow Z\gamma$ ,  $Z \rightarrow ll$ , where  $l = e$  or  $\mu$ , using  $84.6 \text{ pb}^{-1}$  of proton-proton collision at  $\sqrt{s} = 13 \text{ TeV}$  recorded with the ATLAS detector at the CERN Large Hadron Collider. The specific work in this channel is the optimization of  $H \rightarrow Z\gamma$  signal sensitivity and the background component analysis. Some object selection criteria and categorization strategies have been found useful to optimize the sensitivity, and a data-driven method to calculate the portion of main backgrounds has been introduced here.

The second part presents the measurement of photon identification efficiency measurement for ATLAS Run-II. An electron extrapolation method about transforming electron samples to photon samples for photon ID efficiency measurement via shower shape transformations has been introduced and tested.

# Contents

<b>1</b>	<b>Introduction</b>	<b>3</b>
1.1	Searching for Higgs Decay . . . . .	3
1.2	ATLAS Experiment . . . . .	3
1.3	ATLAS Data Analysis with ROOT . . . . .	4
<b>2</b>	<b>H→Z<math>\gamma</math> Search</b>	<b>4</b>
2.1	H→Z $\gamma$ Decay . . . . .	4
2.1.1	H→Z $\gamma$ introduction . . . . .	4
2.1.2	H→Z $\gamma$ Selection . . . . .	4
2.1.3	Monte Carlo samples in use . . . . .	6
2.2	Sensitivity Optimization . . . . .	6
2.2.1	Definition of Sensitivity . . . . .	6
2.2.2	Scanning of Photon Pt Cuts and Isolation Working Points . . . . .	7
2.2.3	Scanning of Di-lepton Mass window . . . . .	7
2.2.4	Run-I Categorization . . . . .	8
2.2.5	Further Study Based on Run-I Categorization . . . . .	8
2.2.6	Conclusion . . . . .	10
2.3	Background Component Analysis . . . . .	10
2.3.1	ABCD data-driven method . . . . .	10
2.3.2	Closure Test with Monte Carlo Sample . . . . .	11
2.3.3	Applying Data in the Calculation . . . . .	11
2.3.4	Conclusion . . . . .	12
<b>3</b>	<b>Photon Identification efficiency measurement</b>	<b>12</b>
3.1	Photon Identification . . . . .	12
3.2	Photon and Zee Selection . . . . .	13
3.2.1	Single Photon Selection . . . . .	13
3.2.2	Tag and Probe Selection . . . . .	13
3.3	Smirnov Transform . . . . .	14
3.4	Closure-test on MC Zee Sample . . . . .	14
3.5	Applying Data in the Measurement . . . . .	15
3.6	Conclusion . . . . .	15
<b>4</b>	<b>Conclusion</b>	<b>16</b>

# 1 Introduction

## 1.1 Searching for Higgs Decay

The Higgs boson is an elementary particle in the Standard Model. It is the quantum excitation of the Higgs field.

In the Standard Model, the Higgs particle is a boson with no spin, electric charge, or colour charge. It is also very unstable, decaying into other particles almost immediately. Although it is hypothesized that the Higgs field permeates the entire Universe, evidence for its existence has been very difficult to obtain. The importance of this fundamental question led to a 40 year search, and CERN's Large Hadron Collider, able to create Higgs bosons and other particles for observation and study.

On 4 July 2012, the discovery of a new particle with a mass between 125 and 127 GeV/c<sup>2</sup> was announced; physicists suspected that it was the Higgs boson. By March 2013, the particle had been proven to behave, interact, and decay in many of the ways predicted by the Standard Model. It was also tentatively confirmed to have even parity and zero spin, two fundamental attributes of a Higgs boson. This appears to be the first elementary scalar particle discovered in nature.

More data are needed to verify that the discovered particle has properties matching those predicted for the Higgs boson by the Standard Model.

## 1.2 ATLAS Experiment

ATLAS (A Toroidal LHC ApparatuS) is one of the seven particle detector experiments (ALICE, ATLAS, CMS, TOTEM, LHCb, LHCf and MoEDAL) constructed at the Large Hadron Collider (LHC). The experiment is designed to take advantage of the unprecedented energy available at the LHC and observe phenomena that involve highly massive particles which were not observable using earlier lower-energy accelerators. It is hoped that it will shed light on new theories of particle physics beyond the Standard Model.

ATLAS is 46 metres long, 25 metres in diameter, and weighs about 7,000 tonnes; it contains some 3000 km of cable. The experiment is a collaboration involving roughly 3,000 physicists from over 175 institutions in 38 countries. It was one of the two LHC experiments involved in the discovery of a particle consistent with the Higgs boson in July 2012.

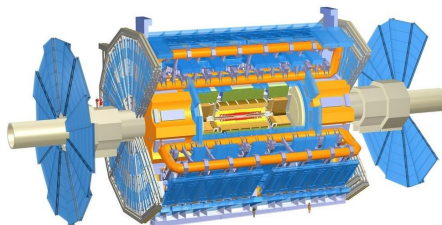


Figure 1: ATLAS Detector

## 1.3 ATLAS Data Analysis with ROOT

ROOT is an object-oriented program and library developed by CERN. It was originally designed for particle physics data analysis and contains several features specific to this field. Parts of the abstract platform are: a graphical user interface and a GUI builder, container classes, reflection, a C++ script and command line interpreter (CINT), object serialization and persistence.

Using ATLAS Analysis Release, one can install ROOT environment, process the event loop and select events from specific physics process like  $H \rightarrow Z\gamma$  from xAOD samples.

ATLAS Collaboration has put the procedures of software installing on twiki website and it's convenient to follow the instructions.

## 2 $H \rightarrow Z\gamma$ Search

### 2.1 $H \rightarrow Z\gamma$ Decay

#### 2.1.1 $H \rightarrow Z\gamma$ introduction

$H \rightarrow Z\gamma$ , is a rare Higgs decay channel which has similar Feynman Diagram(Figure 2) to  $H \rightarrow \gamma\gamma$  process, via Loop Decay.

The Branch Ratio of this channel is comparable to  $H \rightarrow \gamma\gamma$ , but as Z boson continue to decay into two leptons, the cross-section of this channel is more likely to  $H \rightarrow ZZ \rightarrow 4l$ . About 2.3(1.8)fb at 8(7) TeV.

ATLAS RunI Analysis has already covered this decay channel, and gave the limit of its cross-section(Figure 3). As a rare decay channel,  $H \rightarrow Z\gamma$  need more statistical number in RunII, and is hopeful to lead new physics beyond Standard Model.

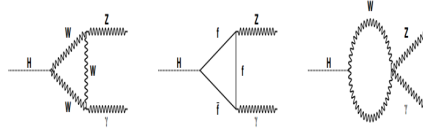


Figure 2: Leading Feynman Diagrams of  $H \rightarrow Z\gamma$

#### 2.1.2 $H \rightarrow Z\gamma$ Selection

The final state of  $H \rightarrow Z\gamma$  process is a high energy photon and two opposite-sign same-flavor leptons(see Figure 4). The selection criteria is based on this final state.

- $\mu$  selection :  $P_t > 10$  GeV,  $|\eta| < 2.7$ . In central barrel  $|\eta| < 0.1$ ,  $P_t > 15$  GeV
- electron selection:  $P_t > 10$  GeV,  $|\eta| < 2.47$  and well reconstructed in ID

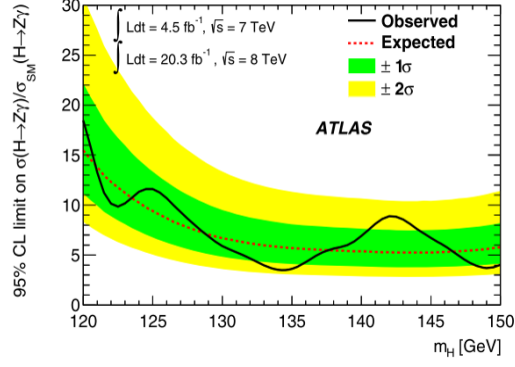


Figure 3: limits on the  $H \rightarrow Z\gamma$  cross-section by Run-I Analysis

- photon selection:  $P_t > 15 \text{ GeV}$ ,  $|\eta| < 1.37$  or  $1.52 < |\eta| < 2.37$
- Rec of Z boson: At least one of two  $\mu$  reconstructed both in ID and MS
- Rec of Z boson: Track and calorimeters isolation requirements
- Rec of Higgs: Z candidate with invariant mass close to Z pole mass
- Rec of Higgs: photon with largest traverse energy are retained
- Rec of Higgs:  $M_{ll} > M_Z - 10 \text{ GeV}$  and  $115 \text{ GeV} < M_{ll\gamma} < 170 \text{ GeV}$
- Further corrections with Final State Radiation and Zmass Constraint

The main Background in this channel is  $Z+\gamma$  and  $Z+\text{jet}$  events, which are 95% of the background events. And there's also some background from Electron-Weak process(5%).

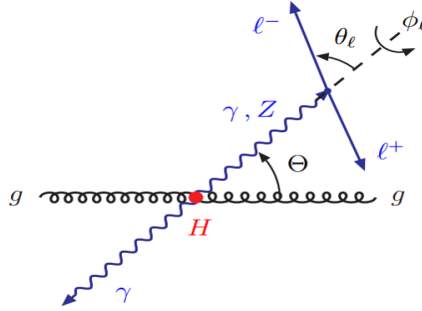


Figure 4: Final State of  $gg \rightarrow H \rightarrow Z\gamma \rightarrow ll\gamma$  Process

### 2.1.3 Monte Carlo samples in use

The samples used to do the following analysis is:

- Data: Data15 13TeV DAOD samples
- Signal MC: MC15 13TeV Higgs(ggH, VBFH, ttH, ZH, WH) DAOD samples
- Background MC: MC15 13TeV Z+ $\gamma$  DAOD samples and Z+jet DAOD samples

The number of Monte Carlo samples has been normalized with current luminosity(84.6pb<sup>-1</sup>), cross-section and total events. From Figure 5 we can tell normalized MC samples and Data match each other. Hence some optimizations can be done by Monte Carlo samples.

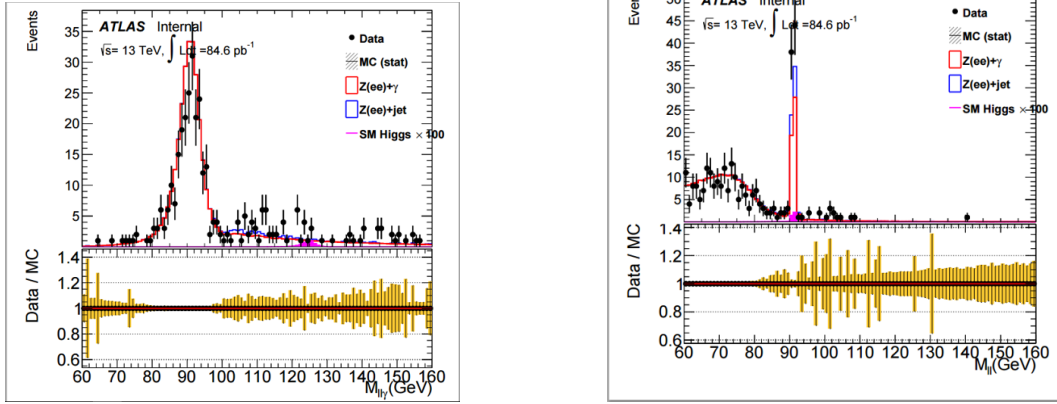


Figure 5:  $l\bar{l}\gamma$  and  $l\bar{l}$  Mass spectrum of Normalized MC sample comparing with Data

## 2.2 Sensitivity Optimization

### 2.2.1 Definition of Sensitivity

Sensitivity is an important attribute of Signal events. We define Sensitivity by the following 2 equivalent formulas  $\text{Sig} = \frac{S}{\sqrt{S+B}}$  and  $\text{Sig} = \sqrt{2[(S+B)\ln\frac{S+B}{B} - S]}$ . We only show the results of the first equation because the 2 equations agree with each other.

Sensitivity Optimization is to scanning selection criteria and categorization strategies to obtain higher signal sensitivity. Before we do the optimization, we define  $120 \text{ GeV} < M_{l\bar{l}\gamma} < 130 \text{ GeV}$  as  $H \rightarrow Z\gamma$  signal region, and apply a tight Photon ID selection on the samples.

### 2.2.2 Scanning of Photon Pt Cuts and Isolation Working Points

Calculating sensitivity via different Object Selection criteria is the first step of the optimization, Table 1 is the sensitivity in different Photon Pt cuts and photon isolation cut working points.

We can draw a conclusion from the table that

- cone20Higgs is the best working point of photon isolation cut, giving 1% to 2% higher sensitivity than other working points.
- Sensitivity when photon Pt > 15 GeV is 9.1% better than photon Pt > 10 GeV
- Sensitivity when photon Pt > 20 GeV is 4.6% better than photon Pt > 15 GeV

We chose our analysis on cone20Higgs isolation working point and photon pt > 15 GeV cuts. A loose cut is used here cause many events will be discard when we use tight cuts in object selection.

ee channel	etcone20	etcone20Higgs	etcone40	etcone40Calo	etcone40<4GeV
Photon Pt > 10 GeV	0.144	0.146	0.144	0.142	0.142
Photon Pt > 15 GeV	0.153	0.155	0.152	0.152	0.153
Photon Pt > 20 GeV	0.161	0.162	0.158	0.160	0.159
Photon Pt > 25 GeV	0.161	0.162	0.156	0.161	0.160

Table 1: Sensitivity in Different Photon Pt Cuts and Isolation Working Points ( $10\text{fb}^{-1}$ )

$\mu\mu$ channel	etcone20	etcone20Higgs	etcone40	etcone40Calo	etcone40<4GeV
Photon Pt > 10 GeV	0.161	0.165	0.163	0.165	0.163
Photon Pt > 15 GeV	0.180	0.184	0.179	0.181	0.180
Photon Pt > 20 GeV	0.187	0.192	0.185	0.187	0.187
Photon Pt > 25 GeV	0.188	0.192	0.185	0.189	0.189

Table 2: Sensitivity in Different Photon Pt Cuts and Isolation Working Points ( $10\text{fb}^{-1}$ )

### 2.2.3 Scanning of Di-lepton Mass window

After object selection, we divide events in different categories, and calculate the combined sensitivity. If the categories is independent to each other, the sensitivity will be much higher. Here we use 4 strategies of categorization:

- Different  $M_{ll}$  mass window
- RunI 8TeV categorization based on  $P_{Tt}$  and  $\Delta\eta_{Z\gamma}$  variables

- Based on RunI categorization, further check the photon converted/unconverted or photon and leptons'  $\eta$  in central/non-central region
- Based on RunI cut base variables(  $P_{Tt}$  and  $\Delta\eta_{Z\gamma}$ ), use a TMVA tool to redo the categorization

Firstly we calculate the sensitivity in different  $M_{ll}$  mass window, scanning the higher and lower limit of  $M_{ll}$ . From Figure 6 we can find sensitivity in  $M_{ll}$  region 80-100GeV is 4.5% better than in 50-135GeV.

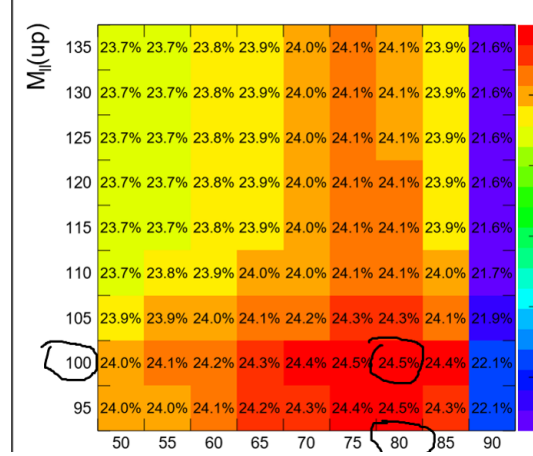


Figure 6: Sensitivity in Different  $ll$  Mass Window

### 2.2.4 Run-I Categorization

Secondly, we divide events in 6 regions using RunI categorization. The specific criteria is:

- High  $P_{Tt}$ :  $P_{Tt} > 30$  GeV
- Low  $P_{Tt}$  High  $\Delta\eta_{Z\gamma}$ :  $P_{Tt} < 30$  GeV,  $\Delta\eta_{Z\gamma} > 2$
- Low  $P_{Tt}$  Low  $\Delta\eta_{Z\gamma}$ :  $P_{Tt} < 30$  GeV,  $\Delta\eta_{Z\gamma} < 2$

From Table 3 we find a 24% better sensitivity than the combined sensitivity of ee and  $\mu\mu$  channels.

### 2.2.5 Further Study Based on Run-I Categorization

And based on RunI categorization we continue to divide events in 12 categories according to:

- photon converted/unconverted



ee- $\mu\mu$ Categories		RunI Categories	
ee	15.7%	ee-High $P_{Tt}$	16.4%
$\mu\mu$	18.8%	ee-Low $P_{Tt}$ High $\Delta\eta_{Z\gamma}$	3.2%
		ee-Low $P_{Tt}$ Low $\Delta\eta_{Z\gamma}$	9.8%
		$\mu\mu$ -High $P_{Tt}$	20.1%
		$\mu\mu$ -Low $P_{Tt}$ High $\Delta\eta_{Z\gamma}$	3.9%
		$\mu\mu$ -Low $P_{Tt}$ Low $\Delta\eta_{Z\gamma}$	11.7%
total	24.5%		30.5%

Table 3: Sensitivity in Run-I Categorization ( $10\text{fb}^{-1}$ )

- photon and leptons'  $\eta$  in central region ( $< 1.37$ ) or not

We find from Table 4 that photon converted/unconverted categorization cannot improve the sensitivity, and there will be a 4.9% improvement dividing events according to photon and leptons' eta.

Beside more categories, a TMVA strategy categorization has also been introduced for

Categories	Converted/Central-eta	Unconv/Non-centr	Sensitivity
Run-I Categories			30.5%
Check Photon's Conversion	15.0%	26.6%	30.6%
Check Photon and Leptons' Eta	26.1%	18.5%	32.0%

Table 4: Further Study Based on Run-I Categorization ( $10\text{fb}^{-1}$ )

the optimization. TMVA tool can process many input cut base variables and output one BDTG variable( see Figure 7). And we can redo the categorization according to this BDTG variable.

Table 5 shows the improvement of TMVA method comparing to RunI categorization.

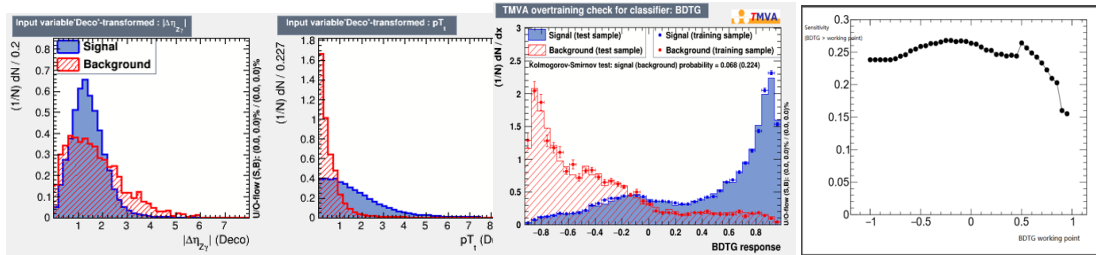


Figure 7: TMVA Method with BDTG variable

The improvement is 6% here.

In further study of sensitivity optimization, more variables and categorization strategies will be applied on this TMVA tool, and a better sensitivity is expected.

Categories	Sensitivity
BDTG > 0.5	26.4%
-0.6 < BDTG < 0.5	18.1%
BDTG < -0.6	5.2%
total	32.4%

Table 5: Sensitivity with TMVA Method ( $10\text{fb}^{-1}$ )

### 2.2.6 Conclusion

We can draw a conclusion here about sensitivity optimization that we can get higher sensitivity by:

- photon  $P_t > 20$  GeV cut
- a  $M_{ll}$  window of 80-100 GeV
- Categorization based on RunI cut base(RunI categorization and TMVA strategy)
- central/non-central  $\eta$  region of photon and leptons

And the optimization will still going on with more variables and categories with TMVA method.

## 2.3 Background Component Analysis

### 2.3.1 ABCD data-driven method

The Background Component Analysis in  $H \rightarrow Z\gamma$  process is mainly to calculate the portion of different backgrounds in this report.

Here the main background is  $Z+\gamma$  and  $Z+\text{jet}$  events( 95% of all the background). So We introduce a data-driven method to control these 2 kinds of events.

The strategy of ABCD Method is shown in Table 6 and Figure 8. Photon tight ID and photon ISO cut is applied to restrained  $Z+\gamma$  events in region A, in the same time, we can obtain the relationship between the  $Z+\text{jet}$  events number in ABCD regions.

$$\frac{Na_{Zjet}}{Nc_{Zjet}} = \frac{Nb_{Zjet}}{Nd_{Zjet}}$$

Then, we can calculate the portion of the 2 samples in Region A, for example  $Z+\gamma$ 's portion is:

$$Purity = 1 - \frac{Nb \times Nc}{Na \times Nd}$$

This equation shows the purity calculation in ideal condition. Actually we must consider the correlation correction of  $Z+\text{jet}$  sample and leakage corrections of  $Z+\gamma$  sample

when calculating the purity. The real solution of purity is in the form

$$Purity \times Na = \frac{-b + \sqrt{b^2 - 4ac}}{2a}$$

where  $a = Cb \times Cc \times R - Cd$ ,  $b = Nd + Cd \times Na - Cc \times Nb \times R - Cb \times Nc \times R$ , and  $c = Nb \times Nc \times R - Na \times Nd$ .

$Cb, Cc, Cd$  and  $R$  are the corrections.

	Photon Tight ID	Photon ISO Cut
RegionA	✓	✓
RegionB	✓	×
RegionC	×	✓
RegionD	×	×

Table 6: Criteria of ABCD Regions

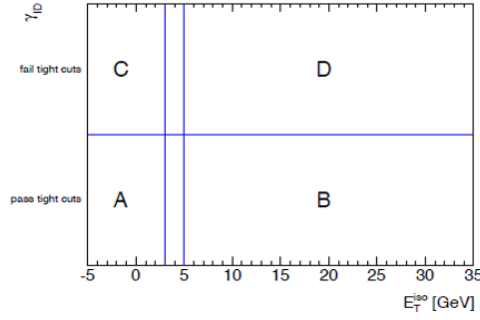


Figure 8: ABCD Data-Driven Method

### 2.3.2 Closure Test with Monte Carlo Sample

Before applying data in the calculation, we add a mixed MC sample on the purity calculation to make sure this method is ready to be used. Cause the mixed MC sample's purity has already be known, we can tell the Purity calculation is ready to be used while input and output purity match each other( Table 7)

### 2.3.3 Applying Data in the Calculation

After the closure text, we use current data sample to do the calculation, the results is in Table 8.

A big statistical uncertainty is shown in the table, we need more statistic number to do the calculation in next steps.

Input Purity	Output Purity(Stat Err)
0.751	0.750 (0.025)

Table 7: Closure Test of Z+ $\gamma$  Purity Calculation

	7TeV-ee	7TeV- $\mu\mu$	8TeV-ee	8TeV- $\mu\mu$	RunII-ee	RunII- $\mu\mu$
Z+ $\gamma$ number	1960	2665	13898	16658	55	76
Purity	0.831	0.866	0.825	0.808	0.554	0.761
Stat Err	0.037	0.030	0.014	0.012	0.384	0.175

Table 8: Purity Calculation with Current Data

### 2.3.4 Conclusion

Purity calculation is ready for usage, but still need more statistic number.

## 3 Photon Identification efficiency measurement

### 3.1 Photon Identification

Photon Identification is a important cut applied in photon selection. The ID efficiency is used to calculate the system uncertainty of the search for all the final states related with photon. And the measurement of Photon ID efficiency can validate the behavior between MC and DATA.

The definition of Photon ID efficiency is the rate photon passes Photon Identification:  $\text{eff} = \frac{N_{\text{passPID}}}{N_{\text{total}}}$ . It's easy to be measured if we have pure photon samples. However, it's very hard to get pure photons via pp collision. So the strategy here is to select the pure electrons samples via Z $\rightarrow$ ee, and transform the electron samples to photon samples.

The algorithms used for photon ID rely on rectangular cuts on calorimeter variables known as "shower shape". Four of many shower shapes is shown in Figure 9. The "transformation" from electrons to photons here, is mainly about transforming the shower shapes.

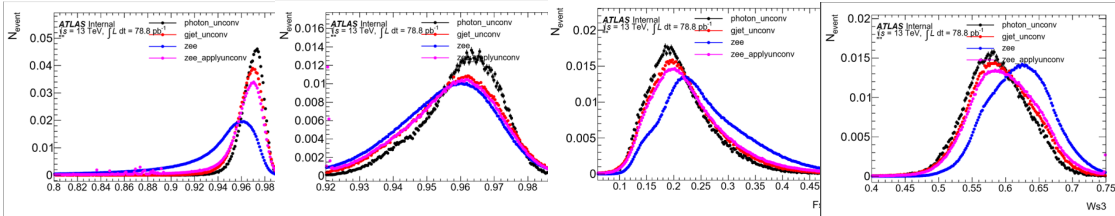


Figure 9: Shower Shape Variables

## 3.2 Photon and Zee Selection

We use MC  $\gamma$ +jet samples to save the photon's shower shape, and use MC Zee samples to save the electron's shower shape. We apply the differences between MC samples on DATA when transforming DATA electrons to DATA photons. The strategy can be seen in Figure 10.

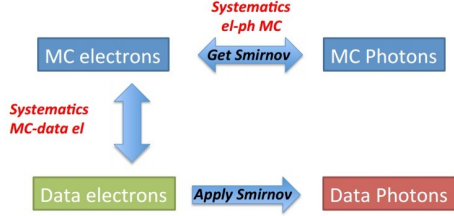


Figure 10: Strategy of Electron Extrapolation Method

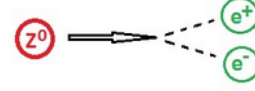


Figure 11:  $Z \rightarrow ee$  Process

### 3.2.1 Single Photon Selection

The criteria of Photon Selection is:

- $P_t > 25 \text{ GeV}$ ;  $|\eta| < 2.37$ , excluding  $[1.37, 1.52]$
- Author: Photon || Ambiguous
- No Fudge Factor, No Photon ID
- Good OQ (collection of 7 object quality cuts)
- $n_{\text{CloseJet}} < 2$  (Jet  $P_t > 20 \text{ GeV}$  and  $\Delta R < 0.4$  is a Close Jet)
- Pass Photon Isolation cut (cone20 working point)
- Truth match ( $\text{status}=1; \text{barcode} < 200000; \text{pdgId}=22; \text{parent} \rightarrow \text{pdgId}() \neq \text{HADRON}$ )

### 3.2.2 Tag and Probe Selection

We use a "Tag and Probe" Selection on Zee sample. It means strict cuts on the tag electron and the reconstruction of  $Z \rightarrow ee$  process. The criteria of  $Z \rightarrow ee$  Selection is:

- $M_{ll}$  range  $80 \text{ GeV} < M_{ll} < 120 \text{ GeV}$
- Two electrons have opposite charge
- The tag electron pass trigger electron ID
- Both electrons  $P_t > 25 \text{ GeV}$ ;  $|\eta| < 2.37$ , excluding  $[1.37, 1.52]$
- Both electrons at least 7 silicon hits and 1 pixel hit
- Less than one Jet  $P_t > 20 \text{ GeV}$  and  $\Delta R < 0.4107$  of the probe electron

### 3.3 Smirnov Transform

The Method we use to transform the shower shapes called "smirnov transform". It's been shown in Figure 12.

In this Figure, the  $R_\phi$  distribution in each sample (top left) is used to calculate the respective Cumulated Density Function (top right). And a Smirnov transformation is derived (bottom left) from different CDFs. We can see the transformed electrons closely resembles the photon distribution (bottom right).

The CDFs on which the process relies are computed from binned distributions, rather than being continuous mathematical functions. For this reason, the calculated mapping is also a non-continuous series of shift values. When applying the transformation to any given value of a shower shape, a linear interpolation is made between the two nearest bins. As a result, there are some imperfections in the transformation which is obtained when applying the method, particularly if the distributions have major discontinuities (small bins are used to minimise any bias from this effect). The ability of the Smirnov transformation to provide a reliable transformation to photon shower shape distributions is thus some-what statistics dependent, and high statistics samples are required for both MC and data. This statistics dependence also limits the extent to which the analysis can be split into separate regions according to variables such as  $p_T$  and  $|\eta|$ .

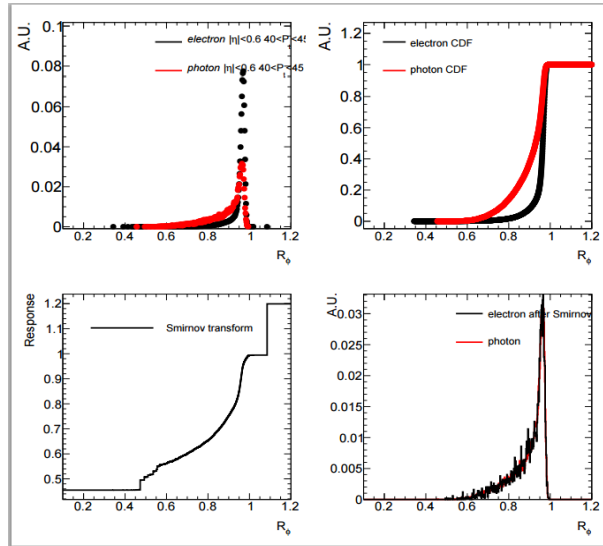


Figure 12: Smirnov Transform

### 3.4 Closure-test on MC Zee Sample

Before we apply the method on data, we also did a closure test here to make sure the transformation is ready to use. The difference between  $\gamma$ +jet sample and Zee samples was applied back to Zee sample in Figure 13. The Pink Points in the Figure are the

transformed Zee sample and the Red Points are  $\gamma$ +jet sample. The transformed Zee sample matched  $\gamma$ +jet sample very well.

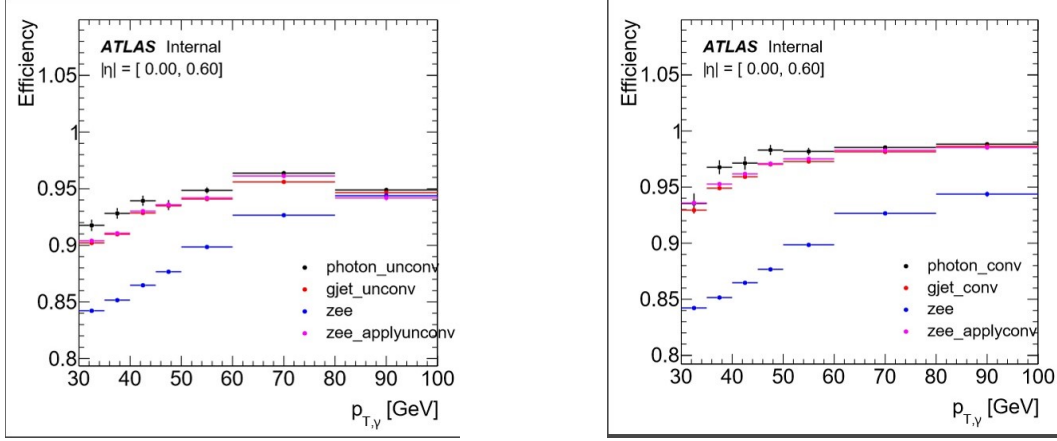


Figure 13: Photon ID Efficiency of Transformed MC Zee sample

### 3.5 Applying Data in the Measurement

After closure test, we apply data on the Photon ID efficiency measurement. Figure 14 is the comparison of transformed MC and DATA Zee events. The MC Photon ID efficiency hasn't match what we obtained in the closure test yet, it need to be further studied. And the statistic uncertainty of DATA is also very large.

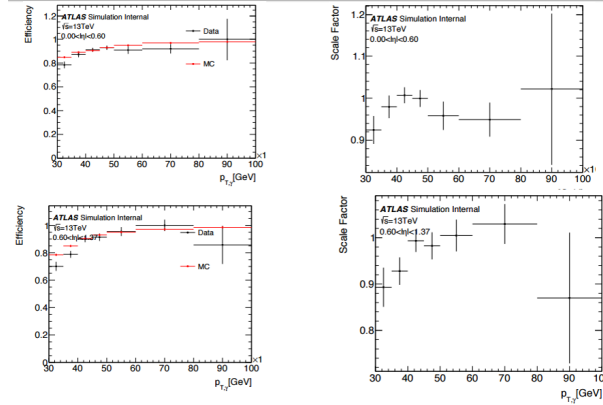


Figure 14: Photon ID Efficiency of Transformed Data Zee events

### 3.6 Conclusion

In Photon ID efficiency measurement, we can draw the conclusion that:

- A electron extrapolation method about using electron samples to calculate photon Id efficiency has been introduced
- Closure test with  $\gamma$ +jet and Zee MC samples has been done. The results match each other. Shower Shape transformation is ready for usage
- Data Zee events do not match MC events quite well while MC events itself is not consistent with what we have in the closure test. We need further study here.

## 4 Conclusion

Firstly, a search for  $H \rightarrow Z\gamma$  has been performed in this report. In the optimization of  $H \rightarrow Z\gamma$  sensitivity. We find specific cuts and categorizations that will be useful to improve the sensitivity.

In background Analysis. We introduced a data-driven method to calculate the portion of different  $H \rightarrow Z\gamma$  background components. This method is ready for usage.

Secondly, The photon ID efficiency measurement with electron extrapolation method has been started. The shower shape transformation is ready for usage, but the Measurement hasn't been consistent between MC and DATA analysis.

The study will go on to:

- More variables and categorization strategies applied to  $H \rightarrow Z\gamma$  optimization
- Calculation of  $Z+\gamma$  portion in  $H \rightarrow Z\gamma$  background with larger DATA
- A full prepared electron extrapolation method for Photon ID efficiency measurement

Thanks to My Supervisor Dr. Yanping Huang, DESY SUMMER SCHOOL, and DESY ATLAS Group!



## References

- [1] ATLAS NOTE(March 6 2014): earch for a Higgs boson in the  $H \rightarrow Z\gamma$  decay mode with  $20.3\text{fb}^{-1}$  of pp collisions at  $\sqrt{s}= 8\text{TeV}$  and  $4.5\text{fb}^{-1}$  of pp collisions at  $\sqrt{s}= 7\text{TeV}$  *T. Barklow, S. Burdin, L. Carminati, J. Cogan, T. Cuhadar Donszelmann, D. Fassouliotis, B. Fulsom, A. Goshaw, H. Hayward, Y. Huang, V. Ippolito, R. Ishmukhametov, R. Kass, B. Lenzi, K. Liu,, Y. Liu, B. Lopez Paredes, J. Loyal, S. Manzoni, G. Marchiori, R.F. Naranjo Garcia, R. Nicolaidou, K. Nikolopoulos, J. Ocariz, S. Paganis, K. Peters, C. Rangel, A. Randle-Conde, N.P. Readioff, S. Sekula, D.Y. Soh, K. Tackmann, J. Tanaka, B. Tannenwald, F. Tian, F. Wang, H. Wang, S. Lan Wu, J. Ye*
- [2] ATLAS NOTE(August 1 2014): Measurement of the identification efficiency of isolated prompt photons in ATLAS by extrapolation from electrons in  $Z \rightarrow$  decays using  $20.3\text{fb}^{-1}$  of pp collisions at  $\sqrt{s}=8\text{TeV}$  *Hengler C, Jimenez M, Tackmann K, Petit E, Gleyzer S, DESY Hamburg (Germany)*